Plastic Deformation and Loss of Joint Force by Creep in High Current Joints

Josef Kindersberger, Helmut Löbl, Stephan Schoft
Technische Universität Dresden,
Germany

Abstract

The paper deals with the numerical simulation of the reduction of joint force in high current aluminum joints and the comparison of the simulation to the results of long-term experiments.
The mechanical stress distribution in aluminum busbar joints is calculated using the Finite Element Method. Based on the physical fundamentals of creep in aluminum the reduction of the joint force by creep depending on the temperature of the joints as well as on the initial joint force and on the washer is simulated. The creep parameters like the Norton exponent and the activation energy of the aluminum under test are determined to fit the results of the simulation to that of the long-term experiments. The effect of retightening the joints on the long-term behaviour of the joint force is studied.

Keywords: electric joints, stress relaxation, creep, FEM simulation

1 Introduction

The aging of electric joints, i. e. the long-term behaviour of the joint resistance is not yet understood completely. However, it is known that four physical mechanisms play an important role in joint aging and contribute to an increasing joint resistance during operating time [1].
Chemical reactions like oxidation or other corrosion processes form highly resistive layers that grow into the a-spots of an electric contact [2], [3], [4].
Interdiffusion in joints made from different conductor materials causes solid solution-, mixed crystal- or intermetallic phases which are mechanically brittle and generally have a higher electric resistivity [5], [6].
Electromigration induced by the electric field and the high current densitiy in the a-spots leads to an atomic mass transport out of the a-spots and results in an increase of the vacancy concentration in the a-spots [1], [7].
Stress relaxation by creep in the conductor- and fittings-material reduces the joint force. The area of the a-spots decreases and causes an increase of the constriction resistance which may occur suddenly, if mechanical vibrations act on the joint [8], [9], [10].
Especially in bolted aluminum busbar joints at high current load, i. e. at high joint temperatures creep may play an important role in joint aging. Previous studies showed that the joint force decreases rapidly at high joint temperatures and leads to sudden increase in joint resistance [8]. To describe the factor of influence of creep on the aging behaviour of high current bolted aluminum busbar joints, the present paper deals with the numerical calculation of the decrease of the joint force based on the fundamentals of creep. The results of simulation are compared to that of long-term experiments.

2 Creep in Metals

The response of a metallic body to mechanical stress σ below the yield stress of the metal results in an instantaneous elastic strain ε_{el}. The yield stress can not be defined as a sharp limit. However, it can be stated that applied stress above the yield stress causes immediate plastic deformation.
Creep in metals, i. e. the time-dependant plastic deformation of metals may occur at mechanical stress well below the yield stress.
The theory of creep describes this phenomenon giving the creep strain rate $\dot{\varepsilon}_{pl}$ depending on the temperature T, on the stress σ, on structural parameters S_i such as dislocation density or grain size and on material parameters P_j such as diffusion constants or the atomic volume [11].

$$\dot{\varepsilon}_{pl} = f(\sigma, T, S_i, P_j) \tag{1}$$

Two major creep mechanisms, i. e. dislocation creep and diffusional creep characterize the time-depending plastic deformation of metals.

2.1 Dislocation Creep

High stress below the yield stress causes creep by conservative motion of dislocations, i. e. glide of dislocations. This motion of dislocations is hindered by the crystal structure itself, i. e. a crystal resistance. Further, discrete obstacles like single solute atoms, segregated particles or other dislocations block the motion of gliding dislocations. At high temperatures obstacle blocked dislocations can be released by dislocation climb. The diffusion of vacancies through the lattice or along the dislocation core into or out of the dislocation core drives the dislocation to change it´s slipping plane and to pass by the obstacle. This non-conservative dislocation motion refers to climb controlled creep [11], [12], [13].

2.2 Diffusional Creep

At low stress the crystal resistance almost inhibits the motion of dislocations. However time dependant plastic deformation at low strain rates takes place by a diffusional flow of atoms.
At low temperatures this diffusional flow occurs as grainboundary diffusion (Coble Creep). At high temperatures the diffusive flow of matter through the lattice becomes dominant (Nabarro-Herring Creep) [11], [12].

The transition between dislocation creep and diffusional creep as well as the transition between dislocation glide and dislocation glide + climb takes place continuously and depends strongly on material parameters.

2.3 Creep Curve

The plot of creep strain depending on time at constant stress can be divided in three characteristic stages.
During the stage of primary creep lasting for some minutes to a few hours initially after applying mechanical stress the creep strain increases rapidly [14].
The second stage of creep, i. e. stationary creep is reached while the dynamic equilibrium of recovery and deformation strengthening is obtained. The creep strain rate is constant and does not depend on time.
The third stage, i. e. the tertiary creep is characterized by an increasing creep rate until the fracture of the material occurs [12].

2.4 Empirical Creep Laws

To describe the creep strain rate depending on temperature, stress and time empirical equations have been proposed [12].
The experimentally proven temperature dependence of the creep strain rate describes creep as thermally activated processes by an Arrhenius law

$$\dot{\varepsilon} \sim \exp\left(\frac{-Q_C}{kT}\right) \tag{2}$$

where k is the Stefan-Boltzmann constant and Q_C is the activation energy depending on the creep mechanism (Table 1).

Table 1: Creep parameters of pure aluminum

	values of pure aluminum from [11]			values used in the simulation
activation energy	dislocation core diffusion Q_C=82kJ/mol	grainboundary diffusion Q_S=84kJ/mol	lattice diffusion Q_L=142kJ/mol	Q_C=44kJ/mol
Norton exponent	diffusional creep n=1	dislocation creep (L.T.) n≈4.4+2	dislocation creep (H.T.) n=4.4	n=4.2

If two or more mechanisms of different activation energies contribute to the creep strain rate the overall activation energy of creep depends on temperature [12]. The activation energy also depends slightly on the mechanical stress by the so called activation volume [13].
The dependence of creep strain rate on time can be described by a power series [12]

$$\dot{\varepsilon} = \sum_i a_i t^{m_i - 1} . \tag{3}$$

Usually a single term of eq. (3) is used to describe the time dependence of the creep strain rate.

$$\dot{\varepsilon} \sim t^{m-1} \tag{4}$$

For primary creep the Andrada creep law is frequently applied using $m = 1/3$. During stationary creep the creep strain rate is constant and m equals 1.
In the range of relatively low and medium stresses the stress dependence of the creep strain rate during stationary state creep is given by the Norton-Bailey creep law

$$\dot{\varepsilon} \sim \sigma^n . \tag{5}$$

The Norton exponent n strongly depends on the creep mechanism and on structural parameters. In the case of diffusional creep the value of n equals 1.
In the case of dislocation creep in pure metals at high temperatures (H.T.-creep) n has a value between 3 and 10 and increases with stress. At lower temperatures (L.T.-creep) core diffusion becomes dominant and a Norton exponent of $n + 2$ is observed. Precipitation or dispersion strengthened metals are usually characterized by n greater than 10 [11], [12].
The creep strain rate generally decreases with the grain size and increases with the density of mobile dislocations.
The kind of stress, i. e. tensile-, compression- or torsional stress does generally not affect the creep behaviour. However, it is reported that in aluminum the creep strain rate differs depending on the kind of stress [15].

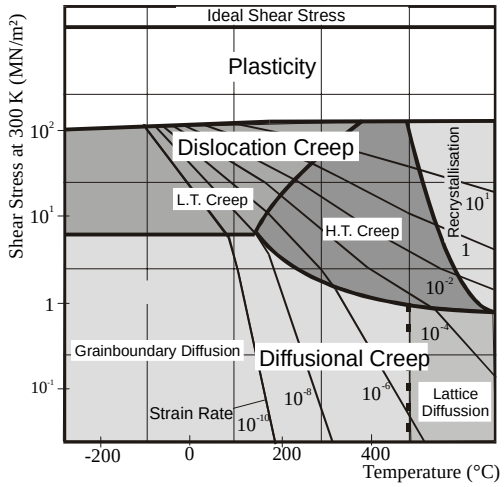

Fig. 1: Creep mechanism map of pure aluminum (grain size d = 10 µm) according to [11]

Deformation mechanism maps have been published for a variety of metals to show which creep mechanism dominates the creep strain rate depending on temperature and stress (Fig. 1) [11]. It shall be noted that these maps are only applicable to the specified material characterized by the grain size, dislocation density and degree of alloying.

3 Material Parameter studies on EAl 99.5

The integral chemical composition of the commercial aluminum used in the longterm studies in the present study was quantified using atomic absorption spectrometry and solution gravimetry (Table 2).

Table 2: Composition of aluminum for electrical use (Wt%)

	Al	Si	Fe	Cu
ANSI H35.1 alloy 1350	>99.5	<0.10	<0.40	<0.05
EN 573-3 EAl99.5 AW-1350	>99.5	<0.10	<0.40	<0.05
Al used in the present study	>99.5	<0.10	0.17	<0.01

The composition of the aluminum used in the present study complies with the ANSI H35.1 and the European Standard of aluminum for electrical use (EN AW-1350 EAl99.5) according EN 573-3 (1994).
The microstructure was studied by optical microscopy. The percentage of iron and silicon occured as segregated particles in an incompletely recrystalized matrix (Fig. 2).

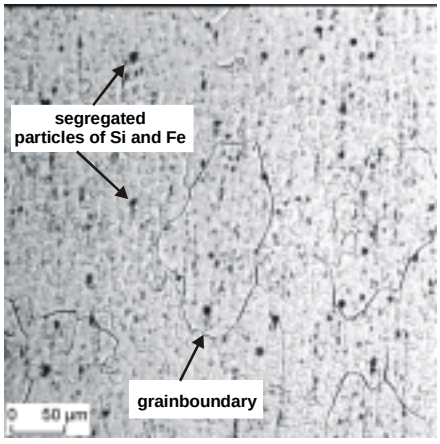

Fig.2 optical microscopy of the microstructure of EAl 99.5 under test

4 Experimental

Six long-term tests on 40 mm x 10 mm x 150 mm electrical busbar joints made from EAl 99.5 as described above were carried out for a period up to 1600 h.
For each test nine busbars were connected in series as a short circuit loop. The overlapping contact areas measuring 40 mm x 40 mm were brushed and cleaned with ethanol shortly before assembly. The current necessary to reach the specified joint temperature T was induced by a high current transformer. The temperature T of the joints was supervised by thermocouples and differed ±2 K from the specified value. The joint force was measured with a mechanical force measuring device using drilled bolts of the dimension M12. A pestle was put into the drill hole and locked in the bolt head. The diplacement of the unstressed pestle related to the stressed bolt shunk was measured with a micrometer gauge [8].
The decrease of the joint force was studied depending on the temperature T of the joints, on the initial joint force $F(0)$, on the outer diameter D and on the thickness h of the washers and on retightening the joints (Table 3).

Table 3: Combinations of test parameters

test N°	joint temperature T [K]	initial joint force $F_j(0)$ [kN]	Dimensions of washers [mm]	retightening after 1000h
1	363	25	D=24, h=2.5	no
2	393	25	D=24, h=2.5	no
3	363	15	D=24, h=2.5	no
4	363	25	D=30, h=5.0	no
5	363	25	D=24, h=2.5	yes

5 Stress Relaxation in Bolted Aluminum Busbar Joints

The decrease of the joint force in bolted aluminum busbar joints occurs by stress relaxation. The model of stress relaxation usually applied to bolted steel joints assumes that the creep strain of the steel bolt $\varepsilon_{Fe,cr}(t)$ increases at the expense of the elastic strain $\varepsilon_{Fe,el}(t)$ of the bolt while the bolted bars do not suffer neither from elastic nor plastic deformation. The total of creep strain $\varepsilon_{Fe,cr}(t)$ and elastic strain $\varepsilon_{Fe,el}(t)$ of the bolt amounts the initial elastic strain $\varepsilon_{Fe,el}(t=0)$ of the bolt and remains constant during creep time.
In bolted aluminum busbar joints the elastic modulus of the aluminum bars (E_{Al} = 70 kN/mm²) is much smaller than the elastic modulus of the bolts (E_{Fe} = 210 kN/mm²). Hence, the initial elastic strain of the aluminum bars after tightening the joints is in the same order of magnitude like the elastic strain of the bolts. Therefore a modified stress relaxation model is proposed to characterize the decrease of the joint force by creep in bolted aluminum busbar joints.
The joint force causes the instantaneous elastic compression of the aluminum bars $\Delta l_{Al,el}(0)$ and the instantaneous elastic extension of the bolt $\Delta l_{Fe,el}(0)$ (Fig. 3).

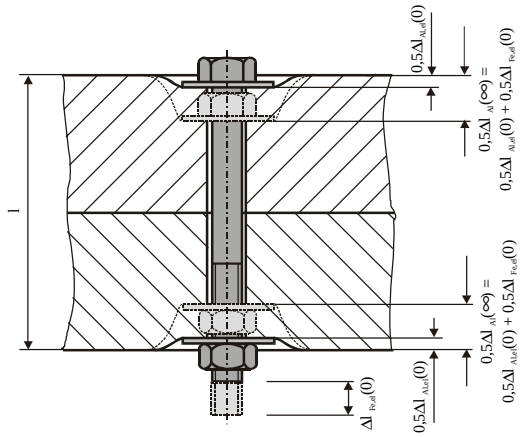

Fig. 3: Geometry of stress relaxation in electric joints (schematic)

During creep time the elastic compression of the aluminum bars $\Delta l_{Al,el}(t)$ decreases and the creep deformation $\Delta l_{Al,cr}(t)$ increases. Assuming that no creep occurs in the bolts' material the compression $\Delta l_{Al}(\infty)$ for infinite time equals the total of the initial elastic expansion of the bolts $\Delta l_{Fe,el}(0)$ and the initial elastic compression of the aluminum bars $\Delta l_{Al,el}(0)$

$$\Delta l_{Al}(\infty) = \Delta l_{Fe,el}(0) + \Delta l_{Al,el}(0)\,. \tag{6}$$

The total compression of the aluminum bars $\Delta l_{Al}(t)$ does not remain constant but increases with time. It equals to the total of the initial elastic extension $\Delta l_{Al,el}(0)$ and the creep deformation of the aluminum bars $\Delta l_{Al,cr}(t)$ depending on time and weighted by a geometry factor (Fig. 4).

$$\Delta l_{Al}(t) = \Delta l_{Al,el}(0) + G\Delta l_{Al,cr}(t) \tag{7}$$

$$G = \frac{\Delta l_{Fe,el}(0)}{\Delta l_{Fe,el}(0) + \Delta l_{Al,el}(0)} \tag{8}$$

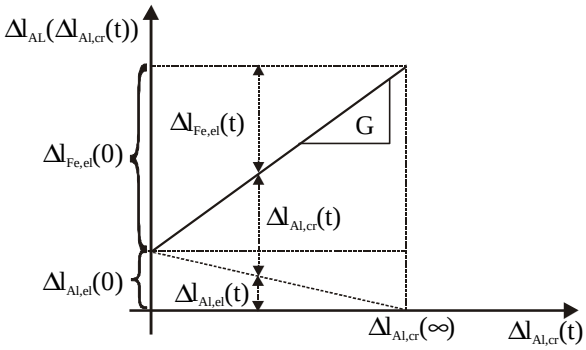

Fig. 4: Total compression of the aluminum bars $\Delta l_{Al}(t)$ as function of the creep deformation of the aluminum bars $\Delta l_{Al,cr}(t)$ during stress relaxation in bolted busbar joints

Eq. (7) written as strain leads to

$$\varepsilon_{Al}(t) = \varepsilon_{Al,el}(t) + \varepsilon_{Al,cr}(t) = \varepsilon_{Al,el}(0) + G\varepsilon_{Al,cr}(t)\,. \tag{9}$$

Introducing Hook´s law results in

$$\sigma_{Al}(t) = E_{Al}\varepsilon_{Al,el}(t) = E_{Al}[\varepsilon_{Al,el}(0) + \varepsilon_{Al,cr}(t)(G-1)]. \tag{10}$$

Differentiating eq. (10) gives the stress rate depending on time

$$\dot{\sigma}_{Al}(t) = E_{Al}(G-1)\dot{\varepsilon}_{Al,cr}(t)\,. \tag{11}$$

Inserting eqs. (2), (4) and (5) into eq. (11) and introducing the proportional constant C leads to the stress rate $\dot{\sigma}_{Al}(t)$ depending on stress σ, time t and temperature T

$$\dot{\sigma}_{Al}(t) = E_{Al}C(G-1)t^{m-1}(\sigma_{Al}(t))^n \exp\left(\frac{-Q_C}{kT}\right). \tag{12}$$

The proportional constant C refers to the microstructure of the aluminum and is generally fitted to measurements.
Solving the differential equation (12) gives

$$\sigma_{Al}(t) = \left[\frac{1-n}{m}E_{Al}C(G-1)t^m \exp\left(\frac{-Q_C}{kT}\right) + \sigma_{Al}^{1-n}(0)\right]^{\frac{1}{1-n}}. \tag{13}$$

Eq. (13) is only applicable to calculate the decrease of mechanical stress in structures with a homogenous stress distribution. It is quite obvious that the stress distribution in bolted busbar joints is inhomogenous. The mechanical stress distribution is calculated using the Finite Element Method (FEM). The fundamentals of creep and stress relaxation mentioned above are implemented in the FE-model and the decrease of the mechanical stress is simulated.

6 *Calculation of the Mechanical Stress Distribution in Bolted Aluminum Busbar Joints*

To calculate the mechanical stress distribution in bolted aluminum busbar joints a two-dimensional FE-model of the joint is build. It is assumed that the stress distribution is rotationally symmetric in respect of the axis of the bolt and mirror symmetric to the overlapping contact areas.

To compare the results of the FEM calculations to those of the experimental creep tests the drill hole through the thread and and the shunk of the measurement bolt is reproduced in the FE-model (Fig. 5).
Boundary conditions are applied in such a way that nodal displacements on the symmetry plane, i. e. the contact area of the aluminum busbar are excluded. The joint force was introduced by displacing the nodes at the bottom of the bolt shunk. Therewith the FE-model respects the above mentioned terms of the modified model of stress relaxation. The maximum mechanical stress in the busbar occurs directly underneath the washer. Applying the parameters of test N^o 1 the maximum normal stress amounts 250 N/mm².

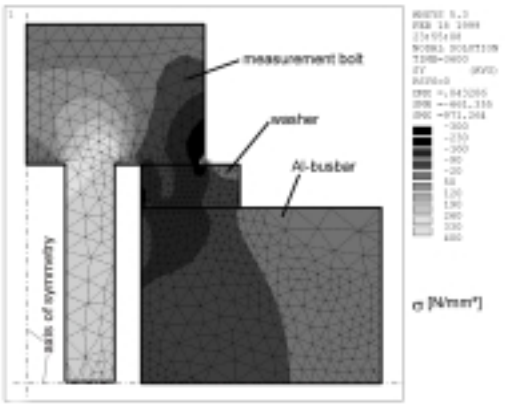

Fig. 5: Mechanical stress distribution in a 40 mm x 10 mm aluminum busbar joint according test N^o 1

7 *Simulation of creep*

To simulate the decrease of the joint force in aluminum busbar joints eq.(12) is applied to the FE-model using ANSYS 5.3 (Fig. 6).

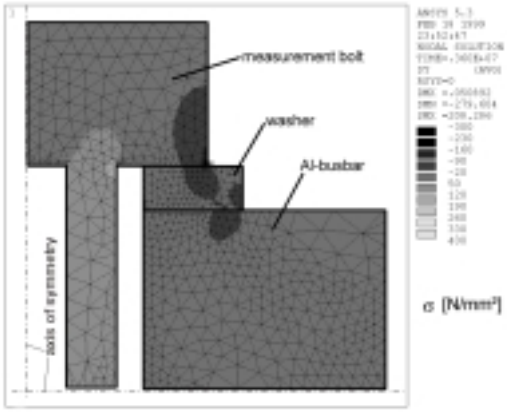

Fig. 6 Stress Distribution after 1000 h, simulation according test N^o 1

The coefficient of thermal expansion of the bolt material ($\alpha_{t,Al} = 0.7 \cdot 10^{-6}\ K^{-1}$) is smaller than that of the aluminum busbar ($\alpha_{t,Al} = 2.4 \cdot 10^{-6}\ K^{-1}$). Therefore, tightening the joints at room temperature and switching on the current leads to a ‚thermal' tightening of the joint. This is simulated by increasing the joint temperature linearly from 293 K to the operating temperature during the first hour of creep simulation.
In the FEM-simulation it is assumed that the Norton exponent n and the activation energy Q neither depend on temperature nor on mechanical stress. This simplification

neglects the fact that due to stress relaxation the volume where dislocation creep occurs decreases with time while the volume where diffusional creep occurs becomes larger.
To simulate the decrease of the mechanical stress primary creep is neglected and only stationary creep is considered to be decisive for the longterm behaviour of the joint force.
The values of the Norton exponent $n = 4.2$, of the activation energy $Q = 44\ kJ/mol$ and of the proportional constant $C = 1.2 \cdot 10^{-9}\ (N/mm^2)^{-4.2}(1/s)$ are choosen to achieve the best fit of the results of simulation to the experimental data in the long-term.
The joint force depending on time is determined by reading out the mean stress at the bottom of the bolt shunk at several points in creep time and plotted in the diagrams of the creep tests.

8 Results and Discussion

The measured data of the creep tests are compared to the results of the FEM-simulation according to the test parameters mentioned in table 3 (figures 7a-e).
Higher joint temperatures strongly increase the creep strain rate (test N° 1 and 2).
The creep strain rate strongly depends on the mechanical stress in the joints and slows down rapidly with decreasing joint force.

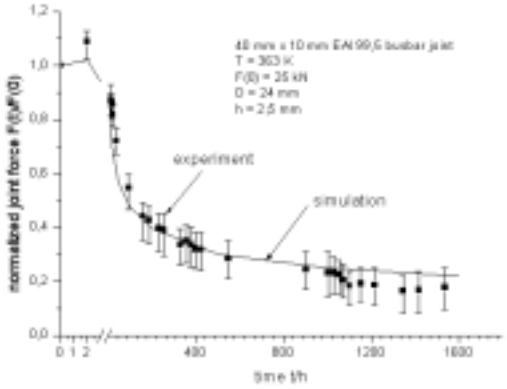

Fig. 7a Development of the joint force at T = 363 K, F(0) = 25 kN, washers: D = 24 mm, h = 2,5 mm

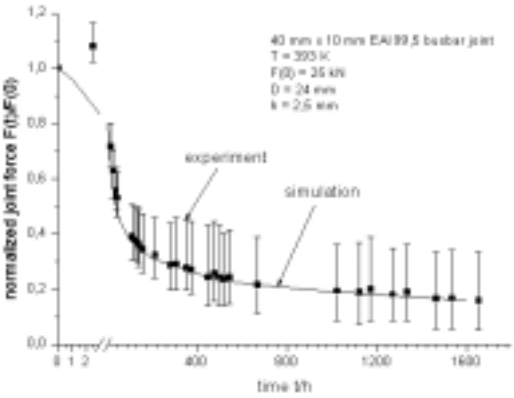

Fig. 7b Development of the joint force at T = 393 K, F(0) = 25 kN, washers: D = 24 mm, h = 2,5 mm

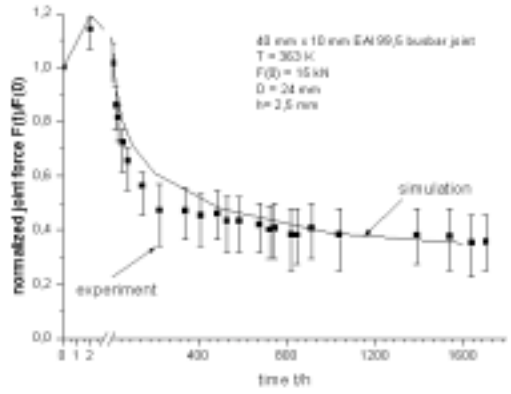

Fig. 7c Development of the joint force at T = 363 K, F(0) = 15 kN, washers: D = 24 mm, h = 2,5 mm

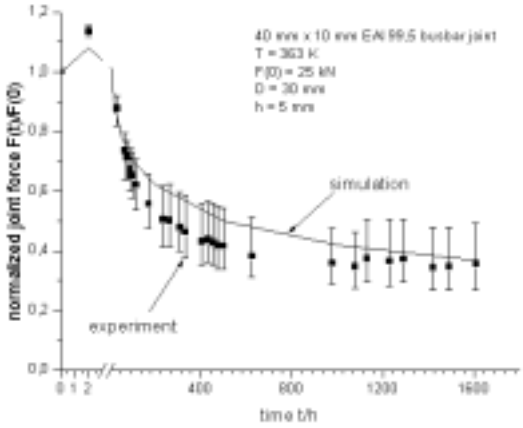

Fig. 7d Development of the joint force at T = 363 K, F(0) = 25 kN, washers: D = 30 mm, h = 5,0 mm

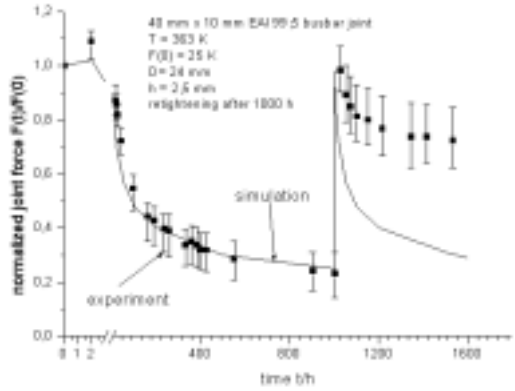

Fig. 7e Development of the joint force at T = 363 K, F(0) = 25 kN, washers: D = 30 mm, h = 2,5 mm, retightening after 1000 h

High initial joint forces cause high creep strain rates just after tightening the joints. Therefore the joint force in joints with high initial joint force approaches the joint force in joints with lower initial joint force (table 4, test N° 1 and 3). However, it shall be noted that the initial joint resistance is decisive for the long-term performance of electrical joints. Due to the hysteresis between the joint force and the joint resistance a sufficient high initial joint force is necessary to obtain a low initial joint resistance and therewith a long lifetime of the joint [8].
Increasing the diameter of the washer leads to a more homogenous stress distribution and therefore to a lower maximum stress in the joints. Hence, the creep strain rate

and the decrease of the joint force are lower than in joints with washers of a minor diameter (test 1 and 4).

Table 4: Decrease of joint force (creep test results)

Test N°	Fig.	F_j(t=0h) mean value	F_j(t=1600h) mean value	ΔF_j	F_j(t=1600h)/ F_j(t=0h)
1	7a	25.0 kN	6.0 kN	19.0 kN	0.24
2	7b	25.0 kN	4.0 kN	21.0 kN	0.16
3	7c	15.0 kN	5.3 kN	9.7 kN	0.35
4	7d	25.0 kN	9.0 kN	16.0 kN	0.36
5	7e	25.0 kN	18 kN	7,0 kN	0.72

Retightening of the joints causes high mechanical stress in the joints and therefore leads to a high creep strain rate just after retightening. The results of the creep tests show that the creep strain rate after retightening is lower than after tightening the joints the first time (test N° 1 and 5). Keeping the above choosen creep parameters this effect can not be reproduced in the simulation.

The stress- and temperature-independant Norton exponent $n = 4.2$ choosen in the simulation is in good accordance to the Norton exponent $n = 4.4$ for H.T. creep in pure aluminum given by literature (table 1). Nevertheless better fit of the experimental data to the simulation is expected using a possibly stress and temperature dependant Norton exponent of the aluminum under test.

The activation energy of 44 kJ/mol found to fit the experimental data amounts 54 % of the lowest activation energy of creep given by literature (table 1). Therefore the activation energy of the aluminum under test has to be studied seperably depending on temperature and stress.

Furthermore it is reported that at high current density the drift electrons may have an effect on the thermally-activated motion of dislocations and may cause lower activation energies of creep by an electroplastic effect [16].

9 Conclusion

The reduction of the joint force in bolted high current aluminum busbar joints was simulated depending on the joint temperature, on the initial joint force, on the washer and on retightening the joints.

- One set of creep parameters has been determined to fit the results of simulation to that of experimental data especially in the longterm behaviour.
- The temperature and the type of washers are the major factors of influence on the long-term behaviour of the joint force.
- The initial joint force does not affect the long-term behaviour of the joint force significantly. Nevertheless a sufficient high initial joint force is essential for a good long-term behaviour of electrical joints provoking a low initial joint resistance.
- Retightening the joints results in an initially higher creep strain rate. However the decrease of the joint force after retightening occurs slower than after tightening the joints the first time.

10 Acknowledegemnts

The authors are grateful to the Deutsche Forschungsgemeinschaft for financial support. Furthermore the authors thank Dr.-Ing. I. Haase and Ing. O. Trommer from the Laboratory of Material Science at Technische Universität Dresden for the optical microscopy and F. Michel from the Institute for Solid State and Materials Research Dresden (IFW) for quantifying the chemical composition of the aluminum alloy used in the tests.

11 References

[1] *Runde, M., Hodne, E., Totdal, B.*: Current-induced Aging of Contact Spots. In: Proceedings of the 35th IEEE Holm-Conference on Electrical Contacts (1989), pp. 213-220

[2] *Lemelson, K.*: Beitrag zur Klärung des Verhaltens geschlossener Starkstromkontaktstellen unter Isolieröl im Dauerbetrieb. Dissertation, Technische Universität Braunschweig, 1973

[3] *Bergmann, R., Böhme, H., Löbl, H., Großmann, S.*: Model to asses the reliability of electrical joints. 18th International Conference on Electrical Contacts (1996), pp. 180-188

[4] Takano, E., Mano, K.: The Failure Mode and Lifetime of Static Contacts. IEEE Transactions on Parts, Materials and Packaging, Vol. PMP-4, N°. 2, (June 1968), pp. 51-55

[5] *Braunovic, M., Aleksandrov, N.*: Intermetallic Compounds at Aluminum-To-Copper and Copper-To-Tin Electrical Interfaces. IEEE Holm Conference on Electrical Contacts (1992), pp. 25-34

[6] *Timsit, R. S.*: Interdiffusion at Bi-metallic Electrical Interfaces. 31th IEEE Holm Conference on Electrical Contact Phenomena (1985), pp. 29-41

[7] *Aronstein, J.*: AC and DC Electromigration in Aluminum Contact Junctions. 18th International Conference on Electrical Contacts (1996), pp. 311-320

[8] *Großmann, S., Kindersberger, J., Löbl, H., Schoft, S.*: Creep Ageing of Bolted Electrical Busbar Joints. 19th International Conference on Electric Contact Phenomena (1998), pp. 269-273

[9] *Braunovic, M.*: Effect of Different Types of Mechanical-Contact Devices on the Performance of Bolted Aluminum-to-Aluminum Joints under Current Cycling and Stress Relaxation Conditions. Holm Conference on Electrical Contacts (1986), pp 133-141

[10] *Stennet, N. A., Campbell, D. S.*: Normal Force Reduction: A Variable Activation Energy Process? 16th International Conference on Electrical Contacts (1992), pp. 191-197

[11] *Frost, H. J., Ashby, M. F.*: Deformation Mechanism Maps. Pergamon Press, Oxford, 1982.

[12] *Cadek, J.*: Creep in metallic materials. Materials Science Monograps, 48, Elsevier, Amsterdam, 1988

[13] *Blum, W.*: High-Temperature Deformation and Creep of Crystalline Solids. Materials science and technology: a comprehensive treatment. VCH, Weinheim, 1993, pp. 359-405

[14] *Mitomi O., Nozawa T., Kawano K.*: Effects of Solder Creep on Optical Component Reliability. IEEE Transactions on Components, Hybrids, and Manufacturing Technology, Vol. CHMT-9, No. 3, (September 1986), pp 265-271.

[15] *Lyssiak, I.*: Kriechen von Konstruktionselementen aus isotropen und anisotropen Werkstoffen mit von der Belastungsart abhängigen Eigenschaften. Thesis, Technische Universität Dresden, 1997

[16] *Sprecher, A. F., Mannan, S. L., Conrad, H.*: On the mechanisms for the electroplastic effect in metals. Acta metall. Vol. 34, N° 7, 1986, pp. 1145-1162